P10.7 THE ROLE OF RESOLUTION IN MODELING THE ARCTIC OCEAN CIRCULATION AND DYNAMICS

Wieslaw Maslowski*[1], Douglas C. Marble[2], Jaclyn L. Clement[1], Waldemar Walczowski[3]
[1]Naval Postgraduate School, Monterey, CA 93943, [2] Fleet Numerical Meteorology and Oceanography Center, Monterey, CA 93943, [3] Institute of Oceanology, Polish Academy of Sciences, Sopot, Poland

1. INTRODUCTION

The Arctic Ocean has been traditionally a challenging region for modeling in part due to the presence of the seasonal and multi-year ice pack and the grid singularity at the North Pole. The bathymetry of this region with the vast shallow shelves, submarine ridges, and troughs and its geometry with narrow straits controlling main exchanges with the North Atlantic (i.e. Fram Strait and Denmark Strait) and the North Pacific (i.e. Bering Strait) has constituted additional complexity for modelers. Finally, the horizontal resolution between 0(1km) and 0(10km) is required to resolve eddies and large scale but narrow boundary currents in the Arctic Ocean.

Regional models of the Arctic Ocean have been developed in part to resolve some of the issues mentioned above. In a partial contribution to the Arctic Ocean Model Intercomparison Project (AOMIP) we compare results of our two coupled ice-ocean models of the Arctic Ocean, configured at 18-km and 30-level (Maslowski et al., 2000, Maslowski et al., 2001) and at 9-km and 45-level grids (Maslowski and Walczowski, 2002, Maslowski and Lipscomb, 2003) (Figure 1). The two models are forced with the same atmospheric fields and were initialized with similar climatological and bathymetry data sets. In addition to the size of the domain and the closed Bering Strait in the 18-km model, notable differences between the two models include the

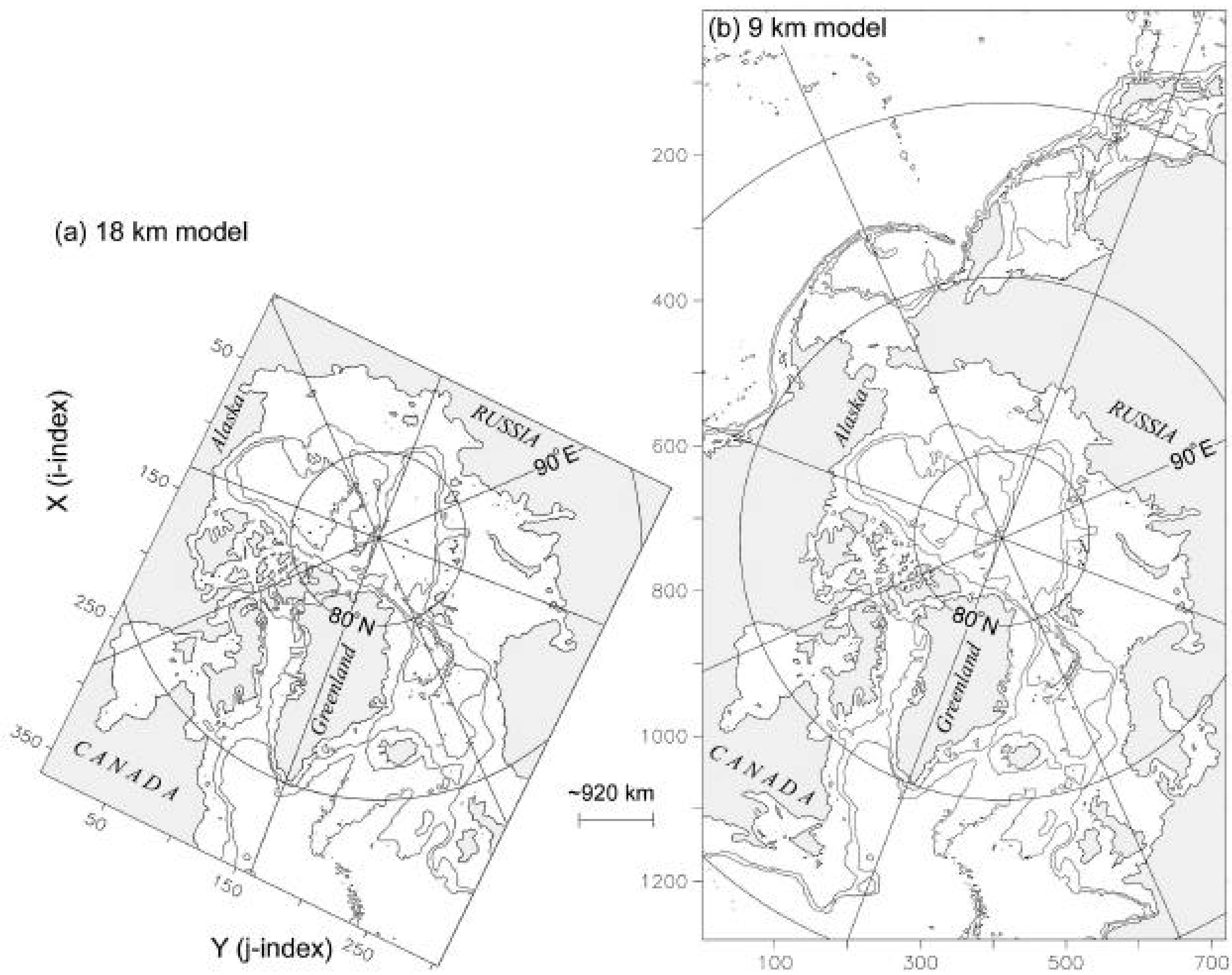

Figure 1. Domain of the (a) 18-km model and (b) 9-km model. The 18-km model image for comparisons is shown rotated 26°. Approximate distance scale is equivalent to 100-9 km model grid points and 50-18 km model grid points. The model 500 and 2500 m isobath contours are shown in black.

Parameter		18 km model	9 km model
ocean model		LANL POP, free surface	LANL POP, free surface
ice model		Hibler (1979)	Hibler (1979)
horizontal grid		368x304	1280x720
vertical levels		30	45
bathymetry		IBCAO+ETOPO	modified ETOPO
initialization fields		PHC 2.0	PHC 1.0
atmospheric forcing		ECMWF	ECMWF
restoring fields	surface	PHC 2.0 monthly mean	PHC 1.0 monthly mean
	Lat. Bdry	PHC 2.0 annual mean	PHC 1.0 annual mean
restoring timescale	surface	Temp-365 d, Sal-120 d	Temp/Sal-30 d
	Lat. Bdry	30 d	10d
timestep	ocean	20 min	8 min
	ice	120 min	48 min
horizontal diffusion coefficients	tracer	-4.00E+18	-5.00E+17
	momentum	-1.00E+19	-1.25E+18
vertical diffusion coefficients	bkgd diff.	0.1	0.05
	bkgd visc.	1	0.2
spinup integration completed		10 yr rpt '79-'93 mean, 3x '79-'81 cycle (9yr)	27yr rpt '79-'93 mn, 6yr rpt '79, 3x '79-'81 cycle (9yr)
diagnostic integration completed		1979-1998	planned 1979-2000
approximate integration time		~28 hr/yr on 64 pe, ARSC T3E-900	~168 hr/yr on 128 pe, ARSC T3E-900

Table 1. Main characteristics of the 18-km and 9-km models, including model configurations and key parameters.

spinup integration, the inclusion of river inputs in the lower resolution model, and bathymetry data used. The summary of the two model characteristics is presented in Table 1.

Results for selected regions of the Arctic region are compared with emphasis on representation of the main circulation features and the mean and eddy kinetic energy. Our findings indicate that the change of model grid resolution not only changes an amount of details represented in a model but more importantly it produces significantly different large scale circulation patterns. Doubling of the horizontal resolution from 18 km to 9 km increases the mean eddy kinetic energy (EKE) in a region by an order of magnitude or more. The knowledge of absolute magnitudes of EKE in the Arctic region is quite limited and further increases of EKE levels in models at even higher resolutions are expected. One of the most significant findings from this work is that inadequately resolving the basic large scale circulation can adversely impact a model's ability to properly represent water mass distributions and interactions due to advection, which will then impact heat, salt and possibly mass balances. Under-representation of eddies and eddy kinetic energy will also impact the transport and mixing of water mass properties. In essence, improvements gained through perfecting sub-grid-scale parameterizations will not help coarser models as improper representation of the circulation will inhibit or prevent water mass interactions. As shown in Seigel et al. (2001), eddy kinetic energy and the generation of eddies increase with increases in resolution, and at higher resolutions the rate of increase slows somewhat. Their highest resolution experiment, a 1.56 km resolution wind-driven, closed-basin, quasi-geostrophic ocean model, is approximately six times the resolution of the 9 km model discussed in this report. This indicates further increases in resolution will continue to result in improvements in the representation of mesoscale and smaller scale processes in the Arctic Ocean. Significance of such findings is discussed in conclusions.

The improvements gained through the increase in resolution can be grouped in the following areas: (1) representation of the bathymetry and circulation in regions where bathymetry is the major controlling factor; (2) the representation of shelf break and coastal boundary currents; and (3) the increase in eddies and eddy kinetic energy noted in the 9 km model. Regional examples in each category will be presented. The data used in the comparisons consist primarily of 1980 annual mean fields. This choice was made as the number of years in which realistic daily varying forcing has been applied to the 9-km model at the time was limited. Every effort has been made to compare equivalent depths and regions. The 9-km model domain is shifted ~26^o to the west when compared to that of 18-

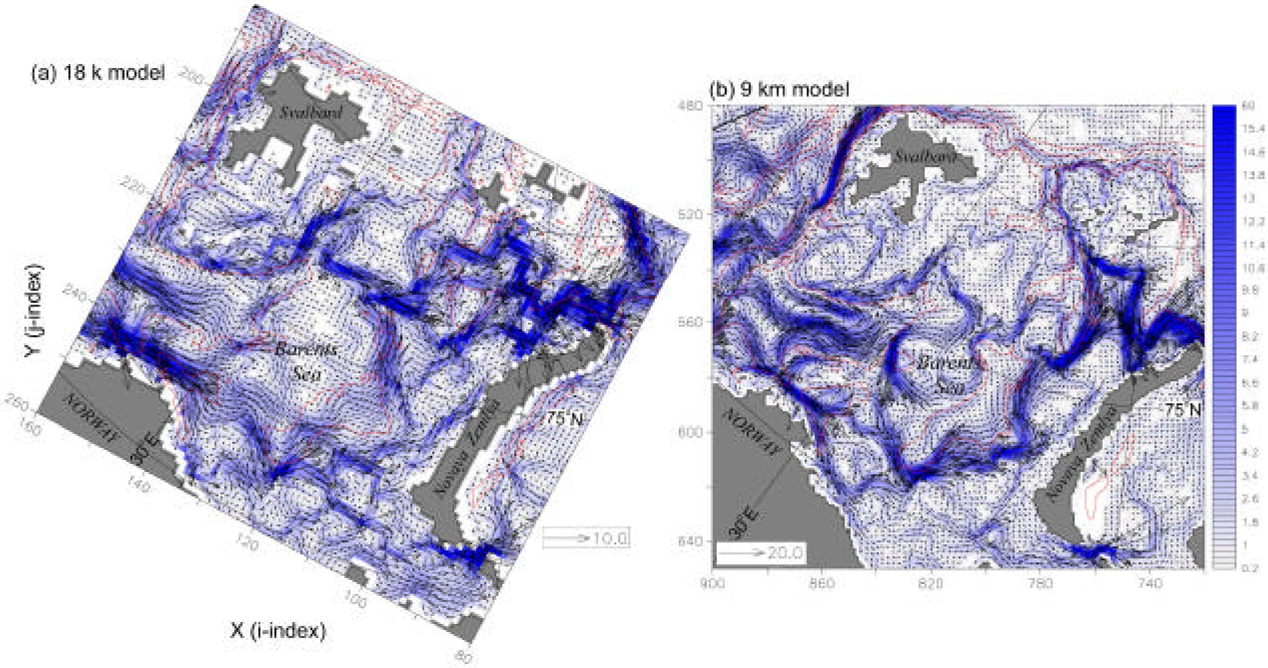

Figure 2. Distribution of 1980 annual mean velocity (cm/s) in the Barents Sea. (a) 18-km model, 0-225 m (model levels 1-7), every vector is plotted; (b) 9-km model, 0-223 m (model levels 1-15), every other vector is plotted. The same background shading of current speed (cm/s) is used for both model images. Note the differing vector scales.

km model. Therefore, 18-km model images, when placed next to 9-km model images, have been rotated 26^o and latitude and bngitude circles are provided for better orientation.

2. BATHYMETRY IMPACTS

It is obvious that increased resolution will result in improved representation of the geography and bathymetry within a model domain. Higher sub-sampling rates along a coastline or a vertical section will capture more details in that profile. Some smoothing will occur and many small features will still be missed but as resolution increases, features attain a more realistic shape. What is less clear is what resolution will ensure enough of the horizontal and vertical variations have been captured to accurately simulate the circulation and mass balances.

The 9-km model exhibits considerable skill in representing the mean circulation in the Barents Sea, a region where bathymetry is a major controlling factor in the circulation (e.g., Pfirman et al., 1994). The 18-km model circulation in the Barents Sea (Figure 2a) exhibits many similar features to the 9 km model. Yet due to poorer vertical resolution and the resultant representation of the bathymetry in the Barents Sea, specifically Great Bank and Central Bank (Figure 2a), the 18-km model displays pathways that are not in agreement with the observed circulation in the Barents Sea (Ozhigin et al., 2000). There appear to be two paths the warm Atlantic Water can follow through the Barents Sea, with larger velocities and more concentrated currents along the northern path (Figure 2a). This dynamical difference has significant physical implications in the nature of the water mass transformation that takes place in the Barents Sea, as it places the primary pathway of warm Atlantic Water through the Barents Sea farther to the north, impacting the oceanic frontal structure as well as the ice edge.

More islands and narrow channels are resolved in the 9-km Canadian Arctic Archipelago when contrasted with the 18-km CAA. The strait between Ellesmere Island and Devon Island, which allows flow out of the Archipelago through Jones Sound, and Prince of Whales Strait, separating Banks Island from Victoria Island are two examples. It appears the main characteristics of Arctic Surface Water outflow through the CAA can be captured by properly resolving the three primary paths: Peary Channel (which includes Viscount Melville Sound and Barrow Strait) to Lancaster Sound; Nares Strait to Smith Sound; and Fury and Hecla Strait to Hudson Strait. However, it was shown that at even 9-km resolution, transports through the Archipelago might be possibly under-represented. One possible solution to this is maintaining the current 9 km resolution and artificially modifying the narrowest points of the three major pathways to achieve the proper transport values. The other solution, which will increase the realism of the circulation through the Archipelago and the representation of eddies and eddy kinetic energy, rather than induce artificiality, is an additional increase in model resolution. The inclusion of the CAA as a nested, higher resolution region within the 9 km model is another option, yet it is felt considerable work remains before nested ocean models achieve the realism and reliability seen in atmospheric models.

3. BOUNDARY CURRENTS

Boundary currents are crucial in the transport of mass, heat, salt and freshwater throughout the Arctic Ocean and the sub-polar seas (Rudels, 1987; Aagaard, 1989, Rudels et al., 1994). The Labrador Sea plays a key role in the global thermohaline circulation as one of the few deep-water formation regions in the world (Broecker, 1991; Skyllingstad et al., 1991). Variations in the transport of cold, fresh Arctic Ocean outflow, as well as sea- ice and icebergs, by boundary currents such as the East and West Greenland Currents, the Baffin Current and the Labrador Current precondition the Greenland Sea and the Labrador Sea for deep convection and deep-water formation.

Large freshwater outflows can severely reduce or cap deep convection in either area (Dickson et al., 1988, 1996), therefore proper representation of these currents is crucial. Labrador Sea boundary currents are narrower and stronger in the 9 km model 1980 annual mean velocity in the top 180 m when compared to the 18 km model (Figure 2). Improved representation of northward flow through Davis Strait is apparent as well as bathymetric effects on the southerly flowing Baffin Land/Labrador Current. The width of the western branch of the Baffin Land/Labrador Current traveling around the 500 m contour at the mouth of Hudson Strait is ~50 km in the 9 km model versus ~100 km in the 18 km model. The separation of the West Greenland Current into several branches of westward flow across the Labrador Sea (as observed, Cuny et al., 2001) is more distinct, as are the interactions between the current along the Labrador coast and the shelf break current. The proximity of the 18 km model boundary and modifications made to the coastline (Figure 1) must be taken into account in the behavior of the coastal current south of 55^{o} N and representation of the northward intrusion of North Atlantic Current meanders into the Labrador Sea (Figure 2a).

4. EDDIES AND EDDY KINETIC ENERGY

Eddies play a significant role in oceanic circulation in that they can result in the propagation of significantly different water masses outside of their place of origination (Gent et al., 1995) and their dissipation transfers momentum between length scales and properties between water masses. Proper eddy parameterization in coarser resolution models is found to be important insofar as eddy-topography interactions contribute to propelling and sustaining narrow boundary currents (Nazarenko et al., 1997; 1998).

Semtner and Chervin (1992) presented results from the first eddy resolving global ocean circulation model and since then, further improvements in the

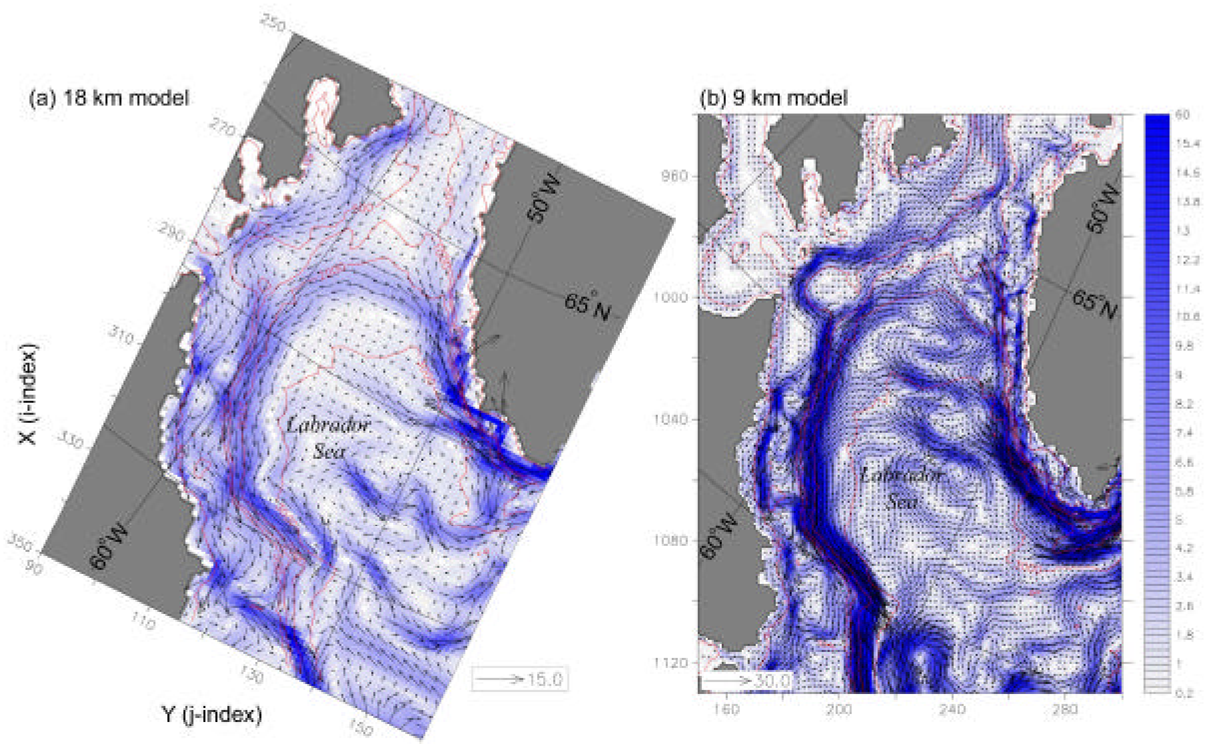

Figure 3. Distribution of 1980 annual mean velocity (cm/s) in the Labrador Sea. (a) 18-km model, 0-180 m (levels 1-6); (b) 9-km model, 0-183 m (levels 1-14). Every other vector is plotted. The same baackground shading is used. Note the differing vector

efficiency of model codes and supercomputer capabilities have allowed continued resolution increases in many applications, which have broadened our view of the intensity and distribution of eddies in the oceans. These resolution increases do come at considerable computational cost (c.f. Table 1 for this limited regional example). There is vigorous and continuing discussion about finding the proper balance between resolution increases and parameterizations which will allow long integrations to accurately simulate circulation at multiple length scales and maintain mass and property balances.

Results presented earlier indicated the 9 km model was able to accurately represent the mean levels of EKE observed in the southern Labrador Sea. Whether the difference between modeled and observed EKE in the northern Labrador Sea is a function of the increased resolution or the significant differences between the atmospheric regime of the early 1980's versus that of the early 1990's adds uncertainty to any conclusions drawn about 9 km model performance in this region. However, comparison of snapshots of EKE in the top ~45 m of the Labrador Sea clearly indicate EKE is significantly under-represented in the 18 km model (Figure 4). The southern maximum in EKE in the 18-km model (Figure 4a) corresponds to energy within a branch of the North Atlantic Current that extends to the north, then east. Geographic distribution of EKE maxima in the 9-km model are in reasonable agreement with the observed means (not shown). The under-representation of EKE in the 18-km model may cause insufficient mixing of water from the West Greenland Current with surface water in the central Labrador Sea. This would in turn impact the degree of stratification, which would affect overturning and deep-water formation.

Dramatic differences exist in the distribution of 0-45 m eddy kinetic energy in the Nordic Seas between the two models as well. When viewed as an aggregate, the concentration of increased EKE in the 9 km model appears to define the path of the North Atlantic Current passing south of Iceland, and the Norwegian Atlantic Current as it travels north, along the west coast of Norway. Indication of such a pathway is absent in the distribution of 18-km model EKE. There is an order of magnitude difference in EKE statistics computed for the regional snapshots discussed previously (Table 2) as well as in the statistics computed for similar regional annual mean surface (0-20 m, 18-km model level 1; 0-5 m, 9-km model level 1) EKE values (not shown).

SUMMARY

Significant improvements in model skill are realized through a doubling of resolution, from 18 km to 9 km. Increasingly realistic bathymetry improves the simulation of topographically steered flows, which in the case of the Barents Sea and other coastal areas can change the regional distribution and transformation of water masses. The inclusion of smaller channels and islands in model Canadian Arctic Archipelago bathymetry results in less artificiality in the simulated flow. However, mass transports remain under-represented even at the higher resolution, suggesting additional increases in resolution might be needed to successfully model this region.

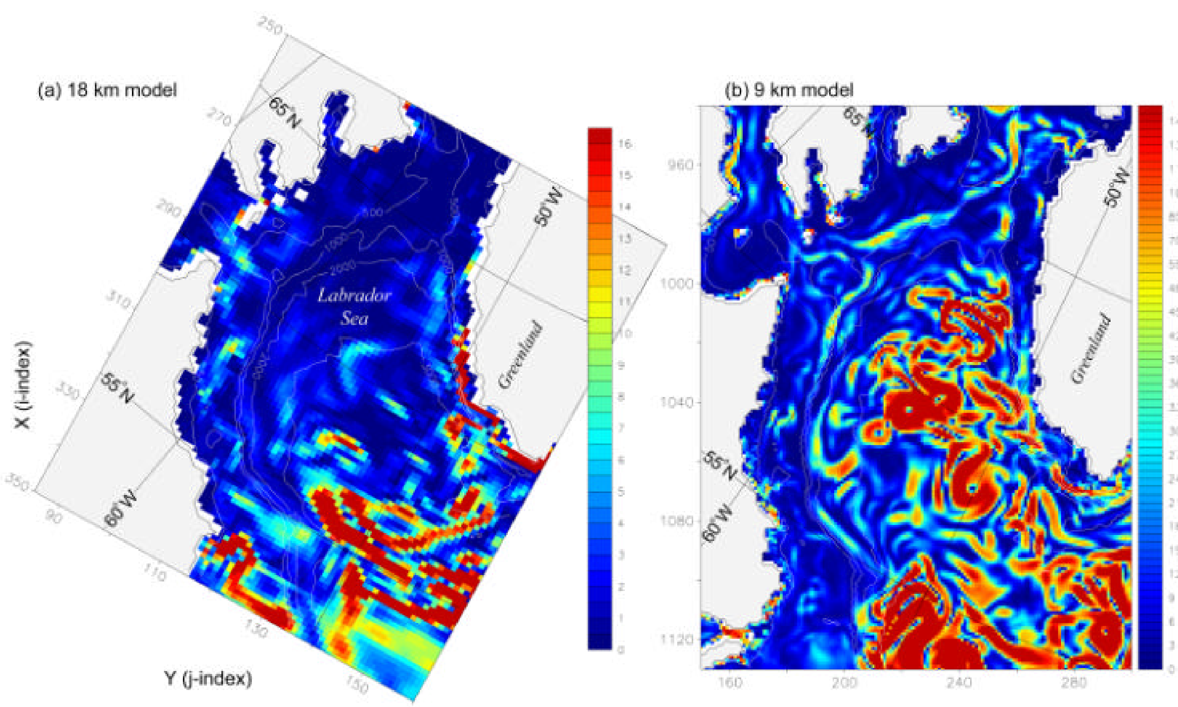

Figure 4. August 1980 snapshot of surface layer eddy kinetic energy (cm^2/s^2) in the Labrador Sea: (a) 18-km model, 0-45 m (model levels 1-2); (b) 9-km model, 0-43 m (model levels 1-7). Note different shading scales.

Model	Labrador Sea EKE			Nordic Seas EKE		
	Maximum	Mean	Std Dev	Maximum	Mean	Std Dev
PCAP58	132.50	4.90	9.20	269.40	4.70	13.30
PIPS	3998.00	70.40	203.70	4959.00	43.50	142.70

Table 2. Eddy kinetic energy (cm^2/s^2) statistics for the 0-45 m regional snapshots.

Boundary currents become narrower and stronger at 9-km resolution and the appearance of opposing boundary currents demonstrates a significant increase in horizontal and vertical shear. The representation of circulation within and around the model Labrador Sea is significantly improved. Better boundary current representation will result in improvements in water mass transport around the perimeter of the Arctic Ocean as well as outflow through the Norwegian and Labrador Seas.

An order of magnitude increase in eddy kinetic energy between the 18 km model and the 9 km model has resulted in simulated values matching observed values in the southern Labrador Sea. The difference between modeled and observed EKE in the northern Labrador Sea is reduced to a factor of two. However, due to the significant differences in the low NAO index atmospheric forcing regime in the early 1980's versus the high NAO regime in the early 1990's (Chapman and Walsh, 1993; Serrezze et al., 1997), model EKE values in the northern Labrador Sea may be closer to observed values than thought. Comparison of modeled EKE values with observed values, as the planned 1979-2000 "hindcast" integration progresses through the early 1990's, will provide a clearer determination.

REFERENCES

Aagaard, K., A synthesis of the Arctic Ocean circulation, in *Reun. Cons. Int. Explor. Mer.*, edited by P.-V. Rapp, pp. 11-22, 1989.

Broecker, W.S., The great ocean conveyor, *Oceanogr.*, *4* (2), 79-89, 1991.

Chapman, W.L., and J.E. Walsh, Recent variations of sea ice and air temperature in high latitudes, *Bull. American Meteorological Soc.*, *74* (1), 33-47, 1993.

Cuny, J., P. Rhines, P. Niiler, and S. Bacon, Labrador Sea boundary Currents and the fate of the Irminger Sea Water, submitted *J. Phys. Oceanogr.* 2001.

Dickson, R.R., J. Meincke, S.-A. Malmberg, and A.J. Lee, The "Great Salinity Anomaly" in the northern North Atlantic 1968-1982, *Progr. Oceanogr.*, *20*, 103-151, 1988.

Dickson, R.R., J. Lazier, J. Meincke, P. Rhines, and J. Swift, Long-term coordinated changes in the convective activity of the North Atlantic, *Progr. Oceanogr.*, *38*, 241-295, 1996.

Gent, P. R., J. Willebrand, T. McDougall, and J. C. McWilliams, Parameterizing eddy-induced tracer transports in ocean circulation models. *J. Phys. Oceanogr.*, *25*, 463-474, 1995.

Maslowski, W., W. Walczowski, 2002: On the circulation of the Baltic Sea and its connection to the Pan-Arctic region – a large scale and high-resolution modeling approach, Boreal Environmental Research, Vol.7, No.4, 319-326.

Maslowski, W., and W.H. Lipscomb: High-resolution Simulations of Arctic Sea Ice During 1979-1993, Polar Research, accepted 2002.

Maslowski, W., B. Newton, P. Schlosser, A. Semtner, and D. Martinson, 2000: Modeling recent climate variability in the Arctic Ocean. Geophys. Res. Lett., 27(22), 3743-3746.

Maslowski, W., D. C. Marble, W. Walczowski, and A. Semtner, 2001: On the large scale shifts in Arctic Ocean and sea-ice conditions during 1979-98. Annals of Glaciology, 33, 545-550.

Nazarenko, L., T. Sou, M. Eby, and G. Holloway, The Arctic ocean-ice system studied by contamination modelling, *Annals Glac.*, *25*, 17-21, 1997.

Nazarenko, L., G. Holloway, and N. Tausnev, Dynamics of transport of "Atlantic signature" in the Arctic Ocean, *J. Geophys. Res.*, *103* (C13), 31,003-31,015, 1998.

Ozhigin, V.K., A. G. Trofimov, and V. A. Ivshin, The Eastern Basin Water and currents in the Barents Sea, in *ICES Annual Science Conference 2000*, 2000.

Pfirman, S.L., D. Bauch, and T. Gammelsrod, The Northern Barents Sea: Water Mass Distribution and Modification, in *The Polar Oceans and Their Role in Shaping the Global Environment: The Nansen Centennial Volume*, edited by O.M. Johannesen, R.D. Muench, and J.E. Overland, pp. 77-94, American Geophysical Union, 1994.

Rudels, B., On the mass balance of the Polar Ocean, with special emphasis on the Fram Strait, *Nor. Polarinst. Skr.*, *188*, 53 pp, 1987.

Rudels, B., E.P. Jones, L.G. Anderson, and G. Kattner, On the intermediate depth waters of the Arctic Ocean, in *The Polar Oceans and Their Role in Shaping the Global Environment: The Nansen Centennial Volume*, edited by O.M. Johannesen, R.D. Muench, and J.E. Overland, pp. 33-46, AGU, Washington, D.C, 1994.

Seigel, A., J. B. Weiss, J. Toomre, J. C. McWilliams, P. S. Berloff, and I Yavneh, Eddies and vortices in ocean basin dynamics, *Geophys Res Lett., 28* (16), 3183, 3186, 2001.

Semtner, A. J., and R. M. Chervin, Ocean circulation from a global eddy-resolving model, *J. Geophys. Res.*, *97*, 5493-5550, 1992.

Serreze, M.C., F. Carse, R. G. Barry, and J. C. Rogers, Icelandic low cyclone activity: climatological features, linkages with the NAO, and relationships with recent changes in the Northern Hemisphere circulation, *J. Climate*, *10*, 453-464, 1997.

Skyllingstad, E.D., D.W. Denbo, and J. Downing, Convection in the Labrador Sea: Community Modeling Effort (CME) results, in *Deep Convection and Deep Water Formation in the Oceans*, edited by P.C. Chu, and J.C. Gascard, Elsevier, New York, 1991.